Electrical Effect of Zinc Nano-Particles on CdS Films grown by slow Solution Process

Mosiori, Cliff Orori[1], Maera, John[2]

[1]Department of Mathematics and Physics, Faculty of Pure and Healthy Sciences, Technical University of Mombasa, P. O. Box 90420 – 80100, Mombasa, Kenya
[2]Department of Physics, Kenyatta University, Box 43844-0100, Nairobi, Kenya

Abstract like CdS, CdSe and CdZnS. In reality, the electric charges that may appear due to certain specific adsorption of the amphoteric hydroxyl group from the complexing agent is assumed to lead to superficial negative charges in the alkaline media of the chemical bath solution and hence positive charges in the acidic chemical bath media. Since the desolating agent is de-ionized water, the nano-particles become charged particles that are peptizable in de-ionized water. But this is only possible with low polarizing counter-ions. When zinc, cadmium and sulphur soluble compound are used, Zn^{+2} and Cd^{+2} with S^{+2} particles formed after co-precipitation in alkaline solution cannot be directly solubilized in water-based growth media. The presence of 'the primary' too polarizing counter-ions such as $(CH_3)NH_3^+$ or NH_4^+ from the complexing agent that remains after the reaction forms a screening effect on charged particles. This consequently reduces charge repulsion between particles and this increases particles aggregate forming doped thin films whose electrical properties are modified as per the level of doping concentration. This research paper investigated the effect of Zinc nano-particles on cadmium sulphide thin film's electrical properties as a function their as-deposited thicknesses. Solution technique was used to grow thin films on ordinary microscope substrate slides from aqueous solutions of Zn^{+2} and Cd^{+2} with S^{+2} ions in the presence of TEA. By varying its deposition time only to obtain eleven (11) samples, resistance was measured using a two point probe while its conductivity type was measured using a Gauss meter as a function of their thicknesses. The thin films were found to be n-type semiconductors with a very high valence electron density, a band gap of 2.43 eV, an average transmittance above 79% on in the VIS - NIR region and a resistivity of $9.5 \times 10^1 - 1.22 \times 10^2$ Ω-cm. Sheet resistivity increased with an increase in Zn ion concentration.

Keywords Nano-particles; Solution technique, Band gap, counter-ions, Complexing Agent, Semiconductor

1. Introduction

The size of a nano-particle is assumed to range between 1 and 100 nm. Studies have shown that metallic nano-particles have different physical and chemical properties from bulk metals (e.g., lower melting points [1-3], higher specific surface areas [4], specific optical properties [5], mechanical strengths [6], and specific magnetizations [7]. These unique properties have attractive various industrial applications. However, how a nano-particle is viewed and defined depends on its specific application. The Zn nano-particles can be prepared by chemical bath technique at room temperature. The reaction bath is possible if it is composed of $ZnCl_2$, NaOH. In this case, TEA (tri ethanolamine) is used as complexing agent. Similarly, many methods can also grow zinc nano-particles. Hence a composite of a non-stoichiometric compound containing zinc, cadmium, and sulfur has attracted research in solar cells [8]. Similar interest has been noted in research areas like photoluminescent [9] and electroluminescent devices [10]. This has been driven by simplicity of this compound to be prepared by solution techniques which are known to allow them to be grown on all kinds of hydrophilic

substrates [11]. It is also a very simple, inexpensive method suitable for applications large area deposition requirements. CdZn$_x$S thin films start from CdS binary thin films [12]. Certain treatments done to binary CdS, such as incorporating Zn onto CdS produces ternary thin films. This third impurity has direct influence on the electrical properties of the resulting material. Some of these properties are useful for applications in single hetero-junction solar cells [13]. In this work, CdS was doped with Zn by varying *x* to produce CdZn$_x$S to lower minority carrier recombination if this material was to be used a window layer in solar cells. The concept used in this work was that the chemical bath deposition of CdS is based on the ion–to– ion model [8] in which growth takes place by condensation of Cd^{+2} and S^{-2} that results in thin film formation. Hence, the growth of CdZn$_x$S thin films results from the incorporation of the Zn ions in the CdS precipitate.

2. Theoretical Considerations

2.1. Resistivity in thin films

Resistance of thin films can be determined by two techniques. The first technique is done by passing a current through a strip of the thin film and then measuring the current and voltage drop on two opposite sides of the film strip. Using the resulting data Ohm's Law is applied to obtain total resistance. The second technique is done by using a four point probe. In this technique, the four probe tip contact are made to be in-contact with the thin film surface from above the coating and then voltage drop between the two middle probe tips and current between the two farthest probe tips is measured. However, in the second technique, an introduction of two correction factors is required, and their values can be obtained from tabulated data in literature on four point probe techniques. Sheet resistance in thin films depends only on thickness. Any change in thickness cause large change in resistance without change of properties. Hence the total resistance [11] is given as:

$$R = R_S \times A \tag{1}$$

where R$_s$ is the surface resistance, A, is the number of squares or from the relation:

$$R = R_s \left(\frac{BW}{Qh^2} + \frac{1}{Qh} - 2(0.46)\frac{B}{Qh} \right) \tag{2}$$

hence;

$$\frac{R_s BW}{nh^2} \approx 1$$

where $Q = \frac{s}{h} + 1$,

where $h = s$ width of each line, *W* is intervals between the lines. This gives resistance as [10]:

$$R = \frac{\rho}{h} \times A \tag{3}$$

2.2. Measurement of Conductivity Type

Optical conductivity (σ_o) is the optical response of a transparent solid. It is given by

$$\sigma_0 = \alpha n \frac{c}{4\Pi} \tag{4}$$

where *c* is the velocity of light. Hence σ_o is the conductivity at the optical frequency concerned and is not generally equal to the direct current (DC) or low frequency conductivity. In metals, σ_o and Π are very high as reflectance approaches unity. In semiconductors Π is usually small, σ_o is reduced and reflectance is also reduced thereby giving higher transparency than in metals. In the case of insulators, Π is very small ($\Pi \rightarrow o$). The dielectric constant ε then tends to n^2 or $n \rightarrow \sqrt{\varepsilon}$. Such measurement is done using the concept of Hall Effect. The Hall coefficient is function of the material and its impurity concentration. Hall Effect is observed when a magnetic field is applied at right angles to a rectangular sample of a material carrying an electric current so that a voltage appears across the sample due to an electric field that is at right angles to both the current and the

applied magnetic field [4]. The the drift field (J_x) cause carriers to flows in the x-direction. The carriers move with an average drift velocity which is vector of Lorentz force as:

$$F = q(E + v \times B) \tag{5}$$

where **F** is the force on the carriers, q is the charge of the carriers, **E** is the electric field acting on the carriers and **B** is the magnetic field. The charge may be positive ("holes") or negative ("electrons"). The total current gives a drift current J_x [14] is given by;

$$J_x = nqv_x \tag{6}$$

where n is the number density and thus we can measure the carrier density in terms of mobility, μ from carrier drift velocity per unit electric field obtained from;

$$v = \mu E \quad \text{or,} \quad \mu = \frac{v_x}{E_x} \tag{7}$$

Giving current density as;

$$J = \sigma E, or \Rightarrow J_x = nqv_x = nq\mu E_x \tag{8}$$

and conductivity σ as [7];

$$\sigma = nq\mu = \frac{1}{\rho} \tag{9}$$

where ρ is the resistivity.

3. Methodology
3.1. Reagents and Chemicals
Analytic grade chemicals of about 99.9% purity including zinc chloride, thiourea, cadmium chloride, absolute ammonia, and triethanolamine (TEA) among others were purchased and used without further purification. Ordinary microscope slides.

3.2. Cleaning of substrates
The microscope slide substrates were prepared and cleaned according to the procedure given by Mosiori *et al.* 2014 and stored for use.

3.3. Experimental Procedures
All solutions were prepared according to Mosiori *et al.,*[12]. The substrate were inserted at a small angle to the vertical and suspended vertically from synthetic foam and the bath composition was maintained at pH of 10. The as deposited films were removed at intervals of 3, 8, 13, 18, 23, 28, 33, 38, 43, 48 and 53 hours to obtain eleven samples as tabulated below respectively cleaned and dried before characterized as deposited for electrical resistivity using a two point probe and a Gauss meter for conductivity type. Therefore the variation x was meant to produce $CdZn_xS$ thin films whose thickness was to vary with growth time.

4. Results and Discussion
4.1. Chemical Process mechanisms
The following formulae were used to calculate the various concentrations of the solutions used;

$$\text{Molarity} = \frac{No.\ of\ moles\ x\ volume\ used}{1000} \tag{10}$$

Concentration as;

$$\text{Concentration} = \frac{mass\ used}{RMM\ x\ 1000} \text{ in moles per litre} \tag{11}$$

The films were cleaned from one side using cotton wool soaked in dilute hydrochloric acid, dried in air and then characterized as-deposited according to Mosiori *et al.* [12]. In the chemical reaction governing the formation of the $CdZn_xS$, the values of x was determined by using the formula;

$$x = \frac{[Zn^{2+}]}{[Cd^{2+} + Zn^{2+}]} \qquad\qquad (12)$$

When the ionic product of Zn^{2+} and S^{2-} exceeds the solubility product ($CdZn_xS$), precipitation starts and overall nuclei start to coagulate onto the substrate [8]. The overall general deposition expression can be represented as:

$$Zn(NH_3)^{2+} + SC(NH_2)_2 + Cd^{2+} + 20H^- \rightarrow CdZn_xS + 4NH_3 + CH_2N_2 + 2H_2O \qquad (13)$$
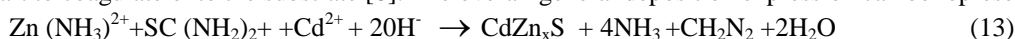
At the initial process, the rate of deposition was high and this was attributed to the high concentrations of Zn^{2+} and S^{2-} in the bath solutions forming a thicker film per unit time spent. As time goes on, precursor solution becomes deficient in ions and this resulted into slower rates of film growth. This work did not achieve the rate of deposition where it is zero or when $S \leq 1$, it was expected if the deposition time as increased to attain terminal thickness hence stopping further deposition.

4.2. Parameters of synthesis
4.2.1. Role of anions
The anions present in the co-precipitation precursor solution of CdZnS as doping takes place has a direct effect on properties the resulting thin film composed of the three metals. Precipitation of individual hydroxides of Cd(II) and Zn(II) ions gives more pure hydroxides in absence of a complexing agent. In the case of Zn, the sequence of anions for obtaining more pure salts is through dissolution in de-ionized water. Therefore, for the formation of Zn (II) particles it is better to take nitrates $Zn(NO_3)_2$ or $ZnCl_2$ as preferable as a compromise. In order to have more equal conditions for all three metals in the whole range of Zn(II) substitution degree $0 \leq x \leq 1$, metals may be taken in the form of their chloride salts.

4.2.2. A rate of mixing of reagents
Co-precipitation consists of two processes: nucleation (formation of centres of crystallization) and a subsequent growth of particles. The relative rates of these two processes determine the size and dispersion of obtained nano-particles as a result of simultaneous formation of new nuclei and growth of the earlier formed particles. Less dispersed in size colloid or thin film is formed when the rate of nucleation is high and the rate of particles growth is low. This situation corresponds to a rapid addition and a vigorous mixing of reagents in the reaction. Slow addition of reagents in the co-precipitation reaction leads to the formation of bigger nuclei than rapid one. This was observed for formation of CdZnS particles [12]. This takes into account the slow addition of the base to solution of metal salts a separate precipitation takes place due to the different pH of precipitation pH for different metals [9]. It is just actual in a two metal system where Cd(II) and Zn(II) as well as in S(II) [14]. It is proposed that separate precipitation may increase the chemical inhomogenity in the particles. To obtain CdZnS particles of a smaller size, well dispersed in size and more chemically homogeneous and uniform mixing of reagents must be performed as fast as possible and for a long time.

4.3. Influence Conditions on the properties
4.3.1. Influence of temperature
An increase in temperature (in the range 20 -35 °C) significantly accelerates formation of CdZnS particles. It is shown for CdZnS particles co-precipitated with TEA as heat increases [13]. For Cd-Zn-S particles with $x = 0.33$ [12] formed at 80 °C the yield of CdZnS estimated that conductivity changes from weak n-type to strong n-type [7]. Their activation energy for formation of Cd-Zn-S of different elements is not equal. Activation energy calculated from kinetics of the formation reactions for two different metals in the temperature range of 20-35 °C decreases in the following sequence: $\mathbf{E_{A(Cd)}} > \mathbf{E_{A(Zn)}} > \mathbf{E_{A(S)}}$ [7]. This sequence is also in agreement with the decreasing of dehydration temperature of the individual hydroxides of the corresponding metals. Many authors [4] conclude that the formation of CdZnS proceeds more readily and starts at lower temperatures. From this discussion, it can be concluded that at room temperature of about 27°C an easier but slow formation of the Cd-Zn-S particles is optimal.

4.3.2. Influence of the pH of the reaction

For the formation of Cd-Zn-S film, the yield grows when the pH of the reaction is increased from 6.8 to 8.6 [6]. Increase of pH value from 8.6 up to 10 leads only to a slight growing of the yield [3]. The most interesting fact is that a further increase of pH up to 13.5-14 leads to a significant growth of the yield but this requires relatively high temperatures of about 75-90 °C [8, 12]. At high pH values the time of formation of Zn ferrite becomes very short [4]. Many authors equally agree and conclude that at high values of pH the reaction of ferrite formation takes place not between solid hydroxides as at pH<10, but between soluble hydroxo-complexes $Zn(OH)_2^-$ and $Cd(OH)_2^-$ in the aqueous state. For formation of $Cd(OH)_2$ (co-precipitating agent) an increase of pH value up to 12.5 accelerates the formation of the CdZnS in a similar manner as for $Zn(OH)_2$. But a further increase of pH up to 14 leads to a reduction of the CdZnS yield. Equally, the variation of the pH value of the reacting solution leads to different size of particles. For $Zn(OH)_2$ at a pH = 8 gives the smallest size of 2 nm and pH = 13 results into the largest size of 6 nm [5]. Formation of the Cd-Zn-S mixed particles optimal pH range is found to be near 12.5 [10].

4.3.3. Influence of the concentration of reagents

No significant difference was found in the yield of Cd-Zn-S when the concentration of metal salts in the co-precipitated reaction is varied from 0.05 to 1 mol -litre on electrical conductivity. Therefore conductivity type depends on the co- precipitated elements. Concentrations of 0.1- 0.2 mol/litre that were taken for the synthesis of CdZnS particles allowed non-viscose primary suspension of particles that was important for better mixing of the reacting volume and hence thin film formation.

4.3.4. Influence of co-precipitating base

The co-precipitating base was found to have a significant influence on the size of obtained CdZnS particles hence an alkaline precursor bath is preferred. For Cd-Zn it has been shown that three different bases give particles with the size diminishing in the following sequence, which coincides with the sequence of reducing strength of the base: $D_{NaOH} > D_{CH_3NH_3OH} > D_{NH_4OH}$ [9]. Attempts to obtain Cd-Zn-S with NH_4OH did not succeed as investigated by other authors [8, 12-13].

4.3.5. Variation of the Zn substitution degree

Size of Cd-Zn-S particles was found to decrease with the increasing of Zn content in the particles [8]. Zn in $CdZn_xS$ particles had sizes of 15.5 nm and - 14.2 nm respectively as determined by Mosiori et al. 2014 [12] and increasing of Zn content leads to a higher amount of associated water in the particles [7] as reported by many authors, the associated water content determined through thermo-gravimetric techniques was found to decrease to a certain level after 24-36 hours of increasing the precursor bath conditions.

4.4. Thin films Sheet Resistivity

A direct current two point probe was used to measure the electrical sheet resistivity, (ρ) in ohm metre (Ω-cm) as a function of thickness. The results were tabulated in table 1 which shows that sheet resistivity decreased exponential from 1.822×10^5 to 0.323×10^5 (Ω-cm) as the film thickness increases from 69 to 300mm. The results were plotted in figure 2.

Table 1: Variation of sheet resistivity with thickness

Sample Label	Thickness (nm)	Resistivity (Ω-cm) x10^5
A	69	1.924
B	120	1.613
C	143	1.262
D	156	0.936
E	166	0.793
F	189	0.736
G	214	0.633
H	237	0.613
I	269	0.542
J	283	0.427
K	300	0.323

This variation in sheet resistivity was attributed to the increase in thickness as well as the increase in Zn concentration in the thin film. Zinc is a good electron conductor and its presence as a dopant increase the degree of conductivity hence the films showed a decrease in resistivity. The presence of Zn was also attributed to crystallinity. The presence of Zn may have improved the relationship of Zn impurities and with CdS crystals in the films. A similar observation was obtained by Mosiori *et al.* [12] who attributed it to the increase in size of crystals that end up modifying resistivity in $Cd_xZn_{1-x}S_x$ thin films [12]. Similar curves were observed by Li, *et al.* [6] and Zong *et al.,* [11] who used different deposition methods but similar reagents.
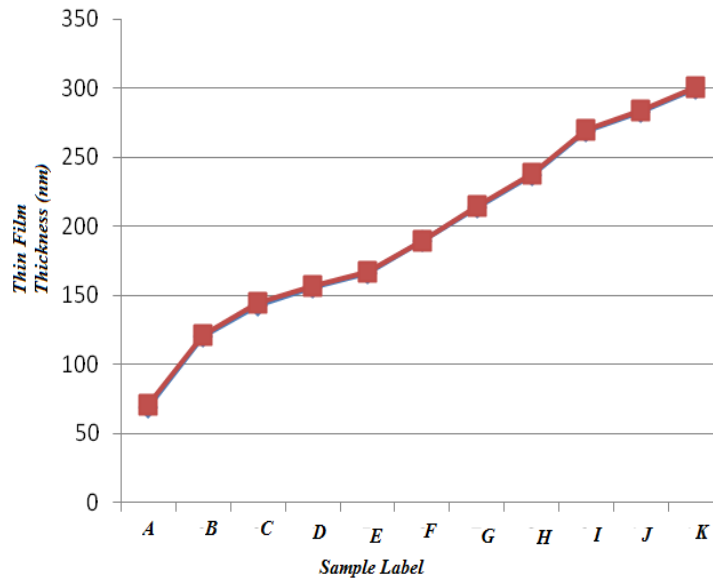

Figure 2: Plot of sheet resistivity against sample label

4.5. Conductivity measurement

The Gauss meter used in this work was programmed to use LabView measure R_H, by controlling the drift current in the samples. The V-I data was recorded from the two volt meters in the gauss meter. The computer labview program was set to have steps of the driving voltage recorded from each of its meters and output the results when the program terminates. The sheet dimensions were set follows: width, (**w**) was set at 0.15 cm, length, (**L**) at 0.37cm = 0.381 cm and thickness of **d** = 166 nm. The choice of thickness was done by assuming that the average thickness was the optimized thin film. Analysis showed that the thin films had intrinsic electron carrier density and hence n-type. This density of valance electrons were calculated as follows [4, 15]: Density of Valence Electrons (DVE) at E_g of 2.41 eV with kT at room temperature being 0.025 eV was;

$$\rho_{electronc} = 7 \times 10^{28}[e^{(-\frac{E_g}{kT})}] = 7 \times 10^{28} \times e^{-96.4} \text{ electrons} \tag{13}$$

Conclusion

In this work, the effect of Zn nanoparticles on CdS forming $CdZn_xS$ (where x was varied) was investigated by solution method on ordinary microscope substrates at room temperature. It influence on electrical properties was discussed and it was found that thickness range from 69 nm to 300 nm and sheet resistivity was dependent on thickness. The thin films were n-type with very high density valence electrons and had an average band gap of 2.41 eV, transmittance of above 79% in the VIS - NIR region with sheet resistivity of 1.924×10^2 - 0.323×10^2 Ω-cm that increased with Zn nanoparticle concentration. The films were proposed to be suitable for solar cell applications.

Acknowledgement

References

[1]. Li, C., Yuan, J., Han, B., Jiang, L., & Shangguan, W. (2010). TiO_2 nanotubes incorporated with CdS for photocatalytic hydrogen production from splitting water under visible light irradiation. International Journal of Hydrogen Energy, 35(13), 7073-7079.

[2]. Wang, L., Wang, W., Shang, M., Yin, W., Sun, S., & Zhang, L. (2010). Enhanced photocatalytic hydrogen evolution under visible light over Cd 1− x ZnxS solid solution with cubic zinc blend phase. International Journal of Hydrogen Energy, 35(1), 19-25.

[3]. Zhang, J., Zhu, Z., Tang, Y., Müllen, K., & Feng, X. (2014). Titania Nanosheet-Mediated Construction of a Two-Dimensional Titania/Cadmium Sulfide Heterostructure for High Hydrogen Evolution Activity. Advanced Materials, 26(5), 734-738.

[4]. Daskalaki, V. M., Antoniadou, M., Li Puma, G., Kondarides, D. I., & Lianos, P. (2010). Solar light-responsive $Pt/CdS/TiO_2$ photocatalysts for hydrogen production and simultaneous degradation of inorganic or organic sacrificial agents in wastewater. Environmental science & technology, 44(19), 7200-7205.

[5]. Yu, J., Zhang, J., & Jaroniec, M. (2010). Preparation and enhanced visible-light photocatalytic H 2-production activity of CdS quantum dots-sensitized $Zn_{1-x}Cd_xS$ solid solution. Green Chemistry, 12(9), 1611-1614.

[6]. Li, Y., Du, J., Peng, S., Xie, D., Lu, G., & Li, S. (2008). Enhancement of photocatalytic activity of cadmium sulfide for hydrogen evolution by photoetching. International Journal of Hydrogen Energy, 33(8), 2007-2013.

[7]. Zhang, K., Jing, D., Chen, Q., & Guo, L. (2010). Influence of Sr-doping on the photocatalytic activities of CdS–ZnS solid solution photocatalysts. International Journal of Hydrogen Energy, 35(5), 2048-2057.

[8]. Mosiori, C., Njoroge, N. and Okumu, J. (2014), Electrical and optical characterization of $Cd_xZn_{1-x}S$ thin films grown by chemical bath deposition in alkaline conditions; Direct Research Journal of Chemistry and Material Science (DRCMS) Vol.2 (1), pp. 13-20, ISSN 2354-4163.

[9]. Kim, D. M., Rahman, M. A., Do, M. H., Ban, C., & Shim, Y. B. (2010). An amperometric chloramphenicol immunosensor based on cadmium sulfide nanoparticles modified-dendrimer bonded conducting polymer. Biosensors and Bioelectronics, 25(7), 1781-1788.

[10]. Jing, D., & Guo, L. (2006). A novel method for the preparation of a highly stable and active CdS photocatalyst with a special surface nanostructure. The Journal of Physical Chemistry B, 110(23), 11139-11145.

[11]. Zong, X., Wu, G., Yan, H., Ma, G., Shi, J., Wen, F., ... & Li, C. (2010). Photocatalytic H_2 evolution on MoS2/CdS catalysts under visible light irradiation. The Journal of Physical Chemistry C, 114(4), 1963-1968.

[12]. Mosiori, C.; Maera, J.; Njoroge, W.; Shikambe, T.; Munji, M.; Magare, R. (**2015**); Modeling Transfer of electrons between Energy States of an Electrolyte and CdS thin films using Gerischer Model - Engineering International; Asian Business Consortium, Issue No: Vol. 3, No. ISSN 2409-3629

[13]. Saravanan, L., Pandurangan, A., & Jayavel, R. (2011). Synthesis of cobalt-doped cadmium sulphide nanocrystals and their optical and magnetic properties. Journal of Nanoparticle Research, 13(4), 1621-1628.

[14]. Li, Y., Hu, Y., Peng, S., Lu, G., & Li, S. (2009). Synthesis of CdS nanorods by an ethylenediamine assisted hydrothermal method for photocatalytic hydrogen evolution. The Journal of Physical Chemistry C, 113(21), 9352-9358.

[15]. Qian, S., Wang, C., Liu, W., Zhu, Y., Yao, W., & Lu, X. (2011). An enhanced CdS/TiO_2 photocatalyst with high stability and activity: effect of mesoporous substrate and bifunctional linking molecule. Journal of Materials Chemistry, 21(13), 4945-4952.